JOURNAL OF MAGNETIC RESONANCE, Series B 102, 317–321 (1993)

A Gradient ^{13}C NOESY-HSQC Experiment for Recording NOESY Spectra of ^{13}C-Labeled Proteins Dissolved in H_2O

D. R. MUHANDIRAM,* NEIL A. FARROW,* GUANG-YI XU,* STEPHEN H. SMALLCOMBE,† AND LEWIS E. KAY*

Protein Engineering Network Centres of Excellence and Departments of Medical Genetics, Biochemistry and Chemistry, University of Toronto, Toronto, Ontario, Canada M5S 1A8; and †Varian Associates, 3120 Hansen Way, Palo Alto, California 94304

Received June 14, 1993

Pulsed field gradients have found a number of important applications in high-resolution protein spectroscopy. Two of the most attractive features of using pulsed field gradients include a reduction in the number of artifacts in multidimensional NMR experiments, where phase cycling is often limited to a small number of steps (*1–4*), and the elimination of the intense solvent signal in H_2O samples (*5–7*).

Our laboratory is developing a family of gradient multidimensional NMR experiments which enable the solution-structure determination of proteins based on data recorded on a single H_2O sample. The use of a single sample to record all of the spectra required for a structure determination has a number of advantages over approaches which require both H_2O and D_2O samples. First, for proteins which cannot be expressed in high yields, there is a considerable cost advantage. Second, the use of a single sample eliminates ambiguities in comparing peak tables from spectra recorded on different samples where the effects of isotope shifts or slight differences in sample conditions can be significant. This has important consequences for automated or semiautomated resonance assignment and structure determination. Recently we have reported pulse schemes for recording HCACO-type spectra (*7*) and HCCH-TOCSY spectra (*8*) on H_2O samples using gradients both to minimize the phase cycling and to eliminate the H_2O signal. In this Communication, we describe a gradient ^{13}C NOESY-HSQC experiment (gd-NOESY-HSQC) which enables the recording of NOE spectra on samples of ^{13}C-labeled protein dissolved in H_2O.

Figure 1 illustrates the gd-NOESY-HSQC sequence that we have developed. The basic pathway of magnetization transfer in the sequence is straightforward and can be outlined by

$$^1H_i(t_1) \xrightarrow{\text{NOE}} {}^1H_j \xrightarrow{J_{HC}} {}^{13}C_j(t_2) \xrightarrow{J_{HC}} {}^1H_j(t_3),$$

where the appropriate transfer mechanisms are given above each arrow, ^1H_j and $^{13}C_j$ are one-bond coupled, and the chemical shifts of ^1H_i, $^{13}C_j$, and ^1H_j evolve during t_1, t_2, and t_3, respectively. In what follows a brief description of the use of gradients in the gd-NOESY-HSQC sequence is presented.

Application of the $90^\circ_{\phi 3}$ ^1H pulse establishes proton transverse magnetization which subsequently evolves during t_1. During the first $t_1/2$ period, evolution of ^1H magnetization due to the large ^1H–^{13}C coupling establishes terms of the form $I_{tr}S_z$, where I_{tr} and S_z denote transverse I and longitudinal S magnetization, respectively. If a perfect ^{13}C 180° pulse is applied at the center of the t_1 evolution period, the effects of ^1H–^{13}C scalar coupling are completely refocused at the end of the t_1 interval. However, many of the spins experience an imperfect pulse due to the large ^{13}C bandwidth as well as RF inhomogeneity effects. This results in the transformation of $I_{tr}S_z$ into zero and multiple-quantum terms. For large molecules, these terms will likely decay completely during the subsequent mixing time; however, the application of the gradient g3 ensures that these terms are completely dephased. If, on the other hand, parts of the sample do not experience the effects of the ^{13}C 180° pulse, terms of the form I_zS_z will be generated following the application of the second ^1H 90° pulse. These terms may not decay completely during T_m and can potentially give rise to artifacts. The application of a ^{13}C 90° pulse during the mixing time followed by a gradient pulse ensures that these terms are completely eliminated.

Gradient pulses g3 and g4 are applied toward the end of the mixing interval T_m to allow radiation damping to restore water magnetization to the $+z$ axis. After the mixing period, application of a 90°_x ^1H pulse reestablishes transverse magnetization. During the subsequent $2\tau_a$ period, proton spins coupled to ^{13}C evolve due to the large one-bond ^1H–^{13}C scalar coupling, and immediately prior to the 90°_y ^1H pulse the magnetization term of interest is of the form I_xS_z, while water magnetization can be described by I_y. The gradient pulse pair (g5, g6) sandwiching the $^1H/^{13}C$ 180° pulses in the middle of the $2\tau_a$ period is applied to eliminate artifacts that might be created by pulse imperfections. In addition, the gradient pair eliminates water magnetization that escapes the ^1H refocusing pulse so that at $2\tau_a$ all of the water mag-

1064-1866/93 $5.00

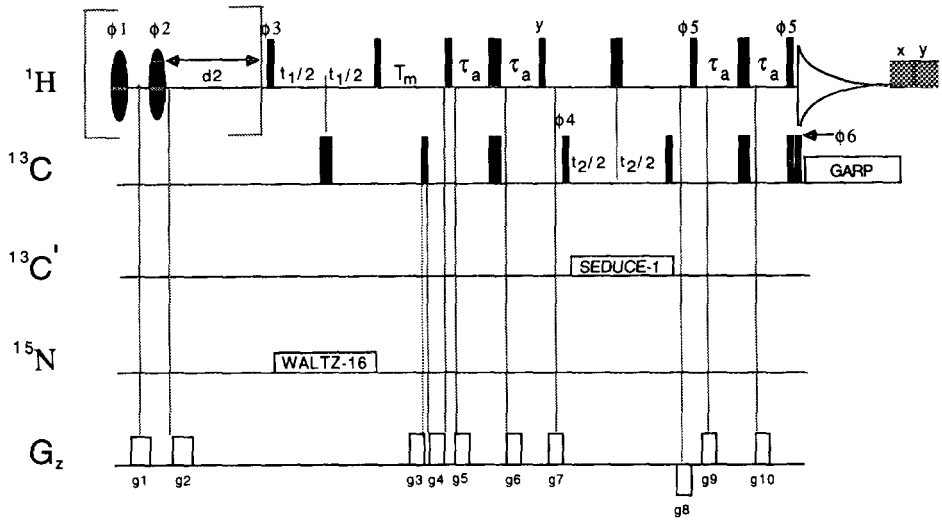

FIG. 1. Pulse sequence of the gd-NOESY-HSQC experiment. Narrow (wide) pulses represent a flip angle of 90° (180°). All ^{1}H hard pulses are applied with a 21.7 kHz field with the carrier set on the water line. Immediately after acquisition, $^1H_{x,y}$ purge pulses are applied, using a 10 kHz field for 8 and 5 ms, respectively. The crafted pulses employed in some of the experiments were 21 ms, with the RF power adjusted for the first pulse to give an on-resonance flip angle of 90°. The second pulse was adjusted in order to minimize the resultant water signal and was typically set to a power level 10 dB greater. The shape profile for the crafted pulses used is given in Ref. (*5*). The ^{13}C pulses were centered at 43 ppm and applied using an 18.5 kHz field. The ^{13}C 180° pulse applied in the center of the t_1 period is of the composite variety ($90^\circ_y 180^\circ_x 90^\circ_y$). C′ decoupling during t_2 was performed with the SEDUCE-1 (*18, 19*) decoupling sequence using a 600 Hz field centered at 175 ppm. Carbon decoupling during acquisition was achieved with GARP (*20*) using a 3.5 kHz field. The GARP decoupling is preceded by a high-power ^{13}C pulse pair as described previously (*21*). ^{15}N decoupling during t_1 was implemented using the WALTZ-16 (*22*) decoupling scheme with a 1 kHz field. The delays used were d2 = 0.1 s, relaxation delay = 0.9 s for experiments where the crafted pulses were used and d2 = 0, relaxation delay = 1.0 s for experiments with no crafted pulses, T_m = 0.15 s, and τ_a = 1.7 ms. The phase cycle used was $\phi_1 = (x, -x)$, $\phi_2 = 2(y), 2(-y)$, $\phi_3 = 4(x), 4(-x)$, $\phi_4 = 8(x), 8(-x)$, $\phi_5 = (x, y, -x, -y)$, $\phi_6 = 4(x), 4(-x)$, Rec = $[x, -y, -x, y, 2(-x, y, x, -y), x, -y, -x, y]$. Phase ϕ_5 was cycled in order to eliminate weak quadrature artifacts in the acquisition dimension. Quadrature in t_1 and t_2 was achieved via States–TPPI of ϕ_3 and ϕ_4, respectively. The durations and strengths of the gradients are: g1 = (10 ms, 2 G/cm), g2 = (8 ms, 4 G/cm), g3 = (3 ms, 15 G/cm), g4 = (1 ms, 20 G/cm), g5 = g6 = (1 ms, 8 G/cm), g7 = (4 ms, 30 G/cm), g8 = (3 ms, −18.8 G/cm), g9 = g10 = (1 ms, 22 G/cm). The gradients are employed in such a way as to maximize the time between the application of a gradient pulse and subsequent application of an RF pulse. A delay of at least 50 μs is found to be necessary in order to avoid sensitivity losses. The crafted pulses are enclosed in brackets to indicate that their use is not essential in this experiment.

netization is along the y axis. This is necessary for the efficient removal of water magnetization by gradient pulses g7 and g8. Subsequent application of a ^{1}H 90°_y pulse creates longitudinal spin order, I_zS_z, for proton spins coupled to ^{13}C, while water magnetization remains in the transverse plane after the pulse and hence is dephased via the action of gradients g7 and g8. It is for this reason that an HSQC rather than an HMQC sequence must be implemented. The use of the longer pulse scheme relative to the ^{13}C NOESY-HMQC sequence (*9*) does not increase the artifact content of the spectra since gradients are employed; however, a slight sensitivity decrease (depending on the RF homogeneity profile of the probe) is experienced due to the increased number of pulses.

It is important to note that gradients g7 and g8 must be applied with opposite polarity since they are separated by a ^{1}H 180° pulse (*2*). If g7 and g8 were of the same polarity and with a perfect ^{1}H 180° pulse in the middle of the t_2 interval, the effects of g7 and g8 with respect to water suppression would cancel. Indeed, in the limit of equal durations, amplitudes, and polarities for g7 and g8, the application of these gradients would not attenuate the water signal at all, neglecting the effects of diffusion. The absolute areas under the gradients g7 and g8 were deliberately set to be different to ensure that water magnetization in regions of the sample not affected by the ^{1}H 180° pulse in the middle of t_2 is not refocused. In addition, potential artifacts that could be created by imperfections in the ^{1}H 180° pulse resulting in the transformation of z operators into transverse operators are eliminated by the application of g8.

It should be noted that in order to minimize relaxation losses which occur during the application of g7 and g8 at a rate given by the decay of the longitudinal ^{1}H–^{13}C spin order, it is important that reasonably strong gradients be applied for short periods of time. Application of the gradient pair (g9, g10) eliminates possible artifacts due to imperfections in the final ^{1}H/^{13}C 180° pulses. The desired magnetization is along the x axis immediately prior to detection while the small residual water magnetization is along the y axis. The final ^{1}H 90°_x pulse has no effect on the desired signal, but serves to rotate any residual water magnetization from the transverse plane to the z axis before acquisition (*7*).

In order to obtain high-resolution protein structures by NMR, it is important that as many NOEs as possible be obtained. This includes NOEs to Hα protons, which frequently resonate at or near the intense H_2O signal. It is therefore crucial that as much of the solvent signal be eliminated as possible. An approach combining the use of gradients and RF pulses is employed to eliminate the intense solvent line. The use of gradients to dephase the water signal while the magnetization of interest is of the form I_zS_z, and hence invariant to the action of the gradients, has been described above. Several additional approaches for water suppression can be employed. Immediately after the detection period, 10 kHz x, y scrambling pulses (*10*) of duration 8 and 5 ms, respectively, are applied. In addition to eliminating any repetition-rate artifacts (*11*), these pulses also aid in water suppression. Following the relaxation delay, during which magnetization recovers to a steady-state value, the water signal can be further suppressed through the application of selective-excitation/gradient pulses as suggested previously by Hurd and co-workers (*5*).

The selective pulses that are employed in the present study are obtained via optimization using the method originated by Shinnar (*12*) and LeRoux (*13*) and are described elsewhere (*5*). The first selective pulse was of duration 21 ms and the power level was adjusted to give a 90° pulse on resonance. This is followed by a gradient pulse to eliminate magnetization that is rotated into the transverse plane by the selective RF pulse. The second selective pulse, also of duration 21 ms, was adjusted in intensity to minimize the water signal. On our spectrometer this is achieved using approximately 10 dB more power for the second pulse. The adjustment of power levels and durations for the shaped pulses is most conveniently achieved using a hard 90°—acquire sequence, preceded by the shaped pulses. The application of the selective pulses and gradients suppresses signals originating from protons resonating at or very close to the water line or from resonances which are in exchange with water. Duration d2 (~100 ms) allows bleached signals to recover via the efficient cross-relaxation pathways which occur in macromolecules in a manner analogous to the SCUBA technique suggested by Mueller and co-workers (*14*). We have found that although the use of the crafted pulses does improve the quality of water suppression, their use is not essential and for this reason the crafted pulses are indicated in parentheses in Fig. 1.

Despite improved water suppression, the crafted-pulse/gradient approach used at the beginning of the sequence does result in a concomitant loss in the intensities of some of the cross peaks. The use of a "mixing" period immediately following the selective pulses partially restores the intensity of these peaks, but at the expense of decreasing the intensities of cross peaks arising from protons that are close in space to the bleached protons. Figure 2 illustrates the effects of the use of the crafted pulses by comparing 2D NOE spectra of

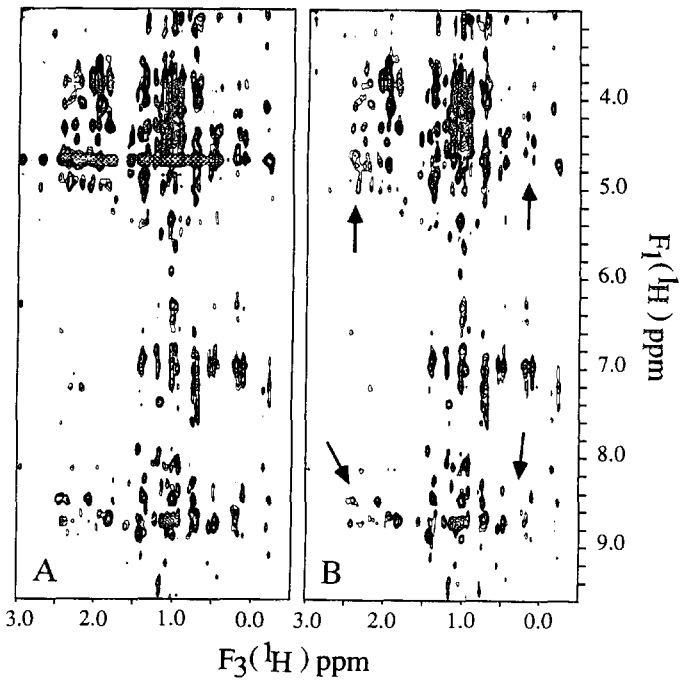

FIG. 2. Comparison of 2D spectra acquired without (A) and with (B) the crafted pulses using the sequence in Fig. 1 with a ^{13}C 180° pulse inserted in the middle of t_2 to ensure that the ^1H–^1H cross-peak intensities are not modulated by the ^{13}C chemical shift of the attached carbons. Each spectrum was acquired with 96 complex t_1 points, 16 transients/t_1 point, a mixing time of 0.15 s, relaxation delay = 1.0 s, d2 = 0 (A) and relaxation delay = 0.9 s, d2 = 0.1 s (B), giving rise to an acquisition time of about one hour. The arrows in (B) point to some of the regions in the spectrum where the use of the crafted pulses has resulted in a decrease in signal intensity.

the *Cellulomonas fimi* cellulose binding domain (CBD; dimer of 110 amino acids/monomer) recorded with the sequence in Fig. 1 without (Fig. 2A) and with (Fig. 2B) the use of such pulses. The spectra were recorded on a sample of 1.5 mM ^{15}N, ^{13}C CBD, 90% H_2O, 10% D_2O, pH 7.0, T = 30°C. The experiments were performed on a Varian UNITY-500 spectrometer equipped with a pulsed-field-gradient accessory and a triple-resonance probe with an actively shielded z gradient. It is clear that certain regions in the spectrum recorded with the use of the crafted pulses are somewhat reduced in intensity. Some of these regions are indicated by arrows in the figure. Another striking difference between the spectra is the appearance of a large number of cross peaks at F_1 = 4.8 ppm, the chemical shift of water in spectra recorded without the crafted pulses. Many of these peaks arise due to NOEs involving labile groups (*15*), such as hydroxy moieties of serine and threonine residues. It is interesting to note that 29 of the 110 residues in CBD are either threonine or serine. In addition, some of the peaks may reflect the presence of bound water molecules (*16*) or may be the result of NOEs with Hα protons which are degenerate with the water resonance.

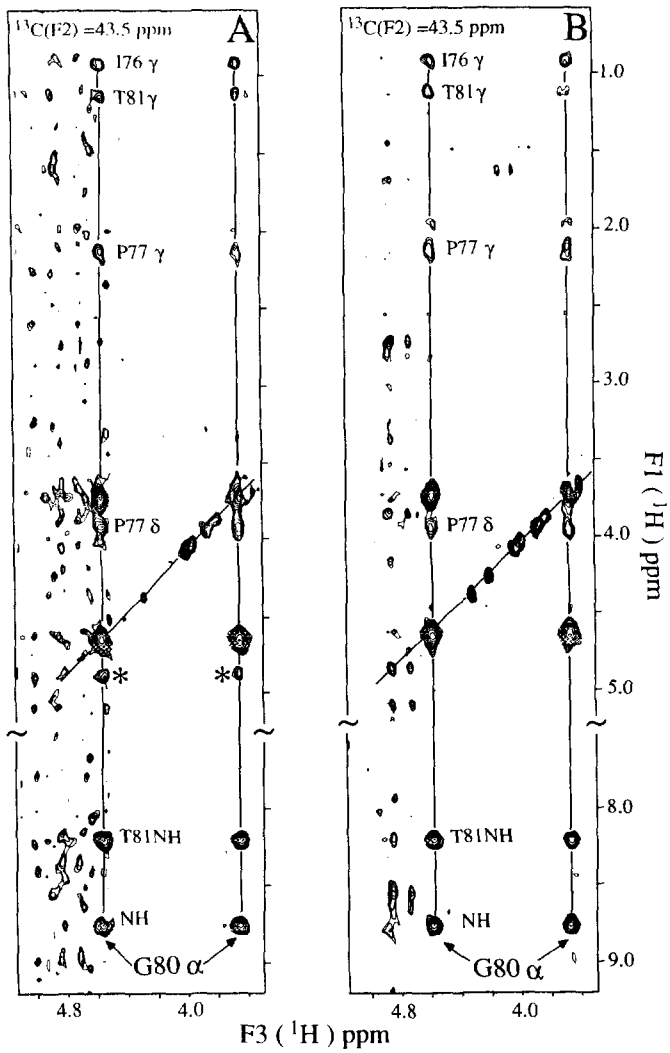

FIG. 3. Slices from 3D ^{13}C gd-NOESY-HSQC data sets at $\delta^{13}C$ = 43.5 ppm acquired without (A) and with (B) crafted pulses on a 1.5 m*M* sample of ^{15}N, ^{13}C-labeled CBD, pH 7.0, 90% H_2O, 10% D_2O, T = 30°C. Both spectra were acquired as 128 × 32 × 416 complex data sets and processed to give absorptive spectra consisting of 256 × 64 × 1024 points in each of (F_1, F_2, F_3). The ^{13}C carrier is set to 43 ppm and a spectral width of 3 kHz is employed. This results in extensive aliasing of resonances. Because a first-order phase correction of 180° is employed in the ^{13}C dimension, both positive and negative cross peaks will be observed. In the figure only positive peaks are shown and the ^{13}C frequency associated with the labeled peaks is indicated in the upper left corner. In both (A) and (B) mixing times of 0.15 s were employed with a relaxation delay of 0.9 s and d2 = 0.1 s (with crafted pulses) or a relaxation delay of 1.0 s (no crafted pulses), giving rise to a total acquisition time of approximately 90 hours for each 3D data set. In both cases residual water was removed using a postacquisition processing procedure described in the text. Cross peaks due to NOEs to water or arising due to NOEs involving exchanging hydroxy groups are indicated with asterisks.

Residual water not eliminated by the gradients can be effectively attenuated in a postacquisition manner using a low-order polynomial fit of the data to remove the low-frequency signals (such as from water on resonance). The fitting procedure was achieved in the following way. Each FID, excluding the region corresponding to the coherence-transfer echo occurring in the 3D time-domain data set at $t_1 = t_3$, was convolved with a boxcar-shaped function and the resulting signal was then fitted to a polynomial of degree 2. The polynomial function optimized in this way was subsequently subtracted from the complete FID to give a spectrum

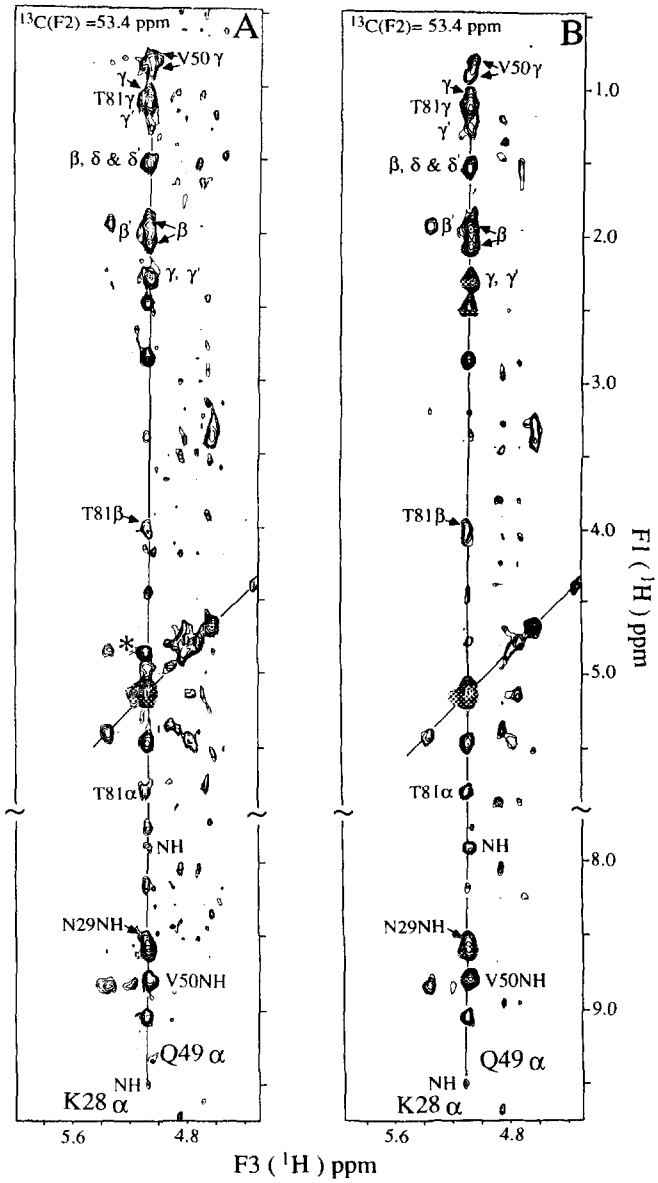

FIG. 4. Slices from 3D ^{13}C gd-NOESY-HSQC data sets at $\delta^{13}C$ = 53.4 ppm acquired without (A) and with (B) crafted pulses. The $^1H\alpha$ and $^{13}C\alpha$ shifts of K28 and Q49 nearly overlap. NOEs to K28α are indicated on the left side of the line through the cross peaks while NOEs to Q49α are indicated on the right side. Intraresidue NOEs are indicated as NH, α, β, etc., while interresidue NOEs are labeled with the appropriate contacts. Only positive peaks are indicated. Cross peaks due to NOEs to water or arising due to NOEs involving exchanging hydroxy groups are indicated with asterisks.

with substantially less residual water. This approach is to be contrasted with the method of Marion *et al.* (*17*), where the convolved FID is subtracted directly from the original FID. Although the residual water signal is very efficiently removed in this latter method, so are many cross peaks to Hα protons.

Figures 3 and 4 illustrate the quality of the data obtained using the gd-NOESY-HSQC sequence without (Figs. 3A and 4A) and with (Figs. 3B and 4B) the use of crafted pulses. The spectra were recorded on the CBD sample under the sample conditions described above. Both data sets were acquired as 128 × 32 × 416 complex data matrices with acquisition times of 25.6 ms (t_1), 10.7 ms (t_2), and 52 ms (t_3). Although the suppression of water is superior where crafted pulses have been employed, even in their absence it is possible to observe NOE peaks to Hα protons with chemical shifts close to water. Unlike the D_2O NOESY experiment, the present experiment also provides NOEs between aliphatic/aromatic and NH protons, as is illustrated in both of the figures. While such NOEs are extremely important in a structure determination, it should be kept in mind that the increased number of magnetization-transfer pathways available to carbon-bound protons in proteins dissolved in H_2O may result in a decrease in the intensity of many of the NOE cross peaks relative to cross peaks in NOESY spectra recorded on samples dissolved in D_2O. The differences in cross-peak intensities for H_2O and D_2O spectra vary depending on the number of transfer pathways available to the protons involved and their relative importance. Included in such pathways are transfers to water molecules. It is interesting to note, for example, the cross peaks to G80α in Fig. 3A at $F_1 \sim 4.8$ ppm that are indicated by asterisks. These cross peaks may be due to NOEs with bound water or may arise as a result of NOEs involving labile groups. Note that these peaks are absent in Fig. 3B (recorded with crafted pulses) and they are also absent in spectra recorded in D_2O.

In summary, we have described a gd-NOESY-HSQC sequence for recording ^{13}C-edited NOESY spectra in H_2O. Although a small amount of residual water remains, it is nonetheless possible to observe cross peaks at least as close as 0.2 ppm from the water. NOEs from all protons in the protein are observed in one experiment using a single H_2O sample. The recording of all data for a structure determination from a single sample should facilitate automated or semiautomated structure determination.

ACKNOWLEDGMENTS

We thank Drs. Warren, Kilburn, and Eng (University of British Columbia) for the generous gift of ^{15}N, ^{13}C-labeled CBD. Valuable discussions with Drs. R. Hurd (GE Medical Systems) and B. John (Varian Associates) are acknowledged. We thank Dr. B. John for kindly providing the intensity vs time profile of the crafted shape used for some of the experiments. This research was supported in part by a grant from the Natural Sciences and Engineering Research Council of Canada.

Note added in proof. In order to achieve more efficient ^{13}C decoupling covering aromatic and aliphatic resonances we now record spectra with the ^{13}C carrier placed at ~67 ppm.

REFERENCES

1. G. W. Vuister, R. Boelens, R. Kaptein, M. Burgering, and P. C. M. van Zijl, *J. Biomol. NMR* **2,** 301 (1992).
2. A. Bax and S. S. Pochapski, *J. Magn. Reson.* **99,** 638 (1992).
3. G. W. Vuister, G. M. Clore, A. M. Gronenborn, R. Powers, D. S. Garrett, R. Tschudin, and A. Bax, *J. Magn. Reson. B* **101,** 210 (1993).
4. D. R. Muhandiram, G. Y. Xu, and L. E. Kay, *J. Biomol. NMR,* in press.
5. B. K. John, D. Plant, P. Webb, and R. E. Hurd, *J. Magn. Reson.* **98,** 200 (1992).
6. B. K. John, D. Plant, and R. E. Hurd, *J. Magn. Reson. A* **101,** 113 (1993).
7. L. E. Kay, *J. Am. Chem. Soc.* **115,** 2055 (1993).
8. L. E. Kay, G. Y. Xu, A. U. Singer, D. R. Muhandiram, and J. D. Forman-Kay, *J. Magn. Reson. B* **101,** 333 (1993).
9. M. Ikura, L. E. Kay, and A. Bax, *J. Magn. Reson.* **86,** 204 (1990).
10. B. A. Messerle, G. Wider, G. Otting, C. Weber, and K. Wüthrich, *J. Magn. Reson.* **85,** 608 (1989).
11. D. Marion, M. Ikura, R. Tschudin, and A. Bax, *J. Magn. Reson.* **85,** 393 (1989).
12. M. Shinnar, S. Eleff, H. Subramanian, and J. S. Leigh, *Magn. Reson. Med.* **12,** 75 (1989).
13. P. Leroux, Abstracts of the Society of Magnetic Resonance in Medicine, 7th Annual Meeting, San Francisco, California, p. 1049, 1988.
14. S. C. Brown, P. L. Weber, and L. Mueller, *J. Magn. Reson.* **77,** 166 (1988).
15. E. Leipinsh, G. Otting, and K. Wüthrich, *J. Biomol. NMR* **2,** 447 (1992).
16. G. Otting and K. Wüthrich, *J. Am. Chem. Soc.* **113,** 4363 (1989).
17. D. Marion, M. Ikura, and A. Bax, *J. Magn. Reson.* **84,** 425 (1989).
18. M. A. McCoy and L. Mueller, *J. Am. Chem. Soc.* **114,** 2108 (1992).
19. M. A. McCoy and L. Mueller, *J. Magn. Reson.* **98,** 674 (1992).
20. A. J. Shaka, P. B. Barker, and R. Freeman, *J. Magn. Reson.* **64,** 547 (1985).
21. A. Bax, G. M. Clore, P. C. Driscoll, A. M. Gronenborn, M. Ikura, and L. E. Kay, *J. Magn. Reson.* **87,** 620 (1990).
22. A. J. Shaka, J. Keeler, T. Frenkiel, and R. Freeman, *J. Magn. Reson.* **52,** 335 (1983).